Pergamon

Chemical Engineering Science, Vol. 53, No. 15, pp. 2839–2857, 1998
© 1998 Elsevier Science Ltd. All rights reserved
Printed in Great Britain
0009–2509/98/$–See front matter

PII: S0009–2509(98)00100–6

Stability of evaporating two-layered liquid film in the presence of surfactant—III. Non-linear stability analysis

Vesselin N. Paunov,* Krassimir D. Danov,* Norbert Alleborn,[†‡] Hans Raszillier[†] and Franz Durst[†]

* Laboratory of Thermodynamics and Physicochemical Hydrodynamics, Faculty of Chemistry, Sofia University, 1 J. Bourchier Ave., 1126 Sofia, Bulgaria

[†] Lehrstuhl für Strömungsmechanik, Universität Erlangen-Nürnberg, Cauerstr. 4, D-91058 Erlangen, Germany

Abstract—In this study we perform non-linear stability analysis of a two-layered liquid film attached to a horizontal solid substrate. The film contains surfactant that is soluble in both liquid phases. The evaporation of solvent from the upper film is also taken into account. The film can exhibit both thermal and surfactant Marangoni instabilities coupled with the effect of the solvent mass loss. The effect due to the van der Waals disjoining pressure is also examined. One particular system is considered: tetrachlorethane–water film upon a PVC plate. We study numerically the influence of surfactant on the film rupture time and the critical film thickness. The role of different factors on the critical thickness and the rupture time is investigated: the intensity of evaporation, the ratio of the thickness of the two layers, the surfactant concentration, and the surfactant distribution coefficient. We demonstrate that the initial perturbations in the squeezing mode are more unstable than the perturbations in the bending mode. It is shown that the effect of surfactant on the film stability is well established. The comparison with the case of pure liquid phases shows that when the surfactant concentration is high enough (tangentially immobile film surfaces) the short and moderate waves are significantly suppressed. Optimal values of the film thicknesses ratio and of the surfactant distribution coefficient are obtained which correspond to maximal stability of the two-layered film against fluctuations. It is found that the results from the linear and non-linear stability analysis differ significantly for the case of pure liquid phases and the differences between them decrease with the increase of the surfactant concentration. © 1998 Elsevier Science Ltd. All rights reserved.

Keywords: Liquid film; stability; evaporation; two layers; soluble surfactant.

1. INTRODUCTION

The stability of multilayered coatings is a problem of great technological importance and scientific interest. The mechanism of arising of instabilities in multilayered liquid films depends on different factors: evaporation or condensation at the upper film interface; disjoining pressure; the presence of surfactant; and the rheological behaviour of the deformed surfactant monolayers. There are numerous contributions to the stability analysis of thin liquid films in the literature [for detailed literature review see Danov *et al.* (1997a, b)].

As known, the linear stability analysis is correct only for small deviations of the film thickness and the surfactant concentration with respect to the basic state (without fluctuations). However, there is no physical limitation of the perturbations magnitude and the film evolution could be strongly influenced by non-linear effects. For example, Williams and Davis (1982) were the first, who performed non-linear stability analysis of laterally unbounded film upon a solid horizontal substrate. They obtained that the rupture time calculated from non-linear analysis can be *several* times smaller than the result from the corresponding linear analysis. Similar results are obtained by Yiantsios and Higgins (1991) for a thin liquid film, bounded by a solid substrate and a second fluid phase semi-infinite in extend. The evolution of well-developed, finite-amplitude waves on a vertically falling film is investigated by Chang (1987). Lee and Mei (1996) described the non-linear waves on the surface of a thin film flowing down an inclined plane at high Reynolds and moderate Weber numbers. A full-scale numerical study of interfacial instabilities

[‡] Corresponding author.

in thin-film flows is performed by Rasmaswamy *et al.* (1996).

There are two ways for generalization of these investigations for practical systems: by including the temperature gradient effects, and by taking into account the real surfactant distribution in that systems. The linear stability and the non-linear evolution equations for thin liquid films with insoluble surfactant are studied by many authors (see e.g. Hatziavramidis, 1992; De Wit *et al.*, 1994; and Paulsen *et al.*, 1996). The interaction between cells and a solid support in aqueous solution can be modelled by considering the stability of the thin aqueous film between them. The non-linear analysis of these systems is given by Gallez (1994), taking into account the formation of specific interactions at short distances. The influence of the evaporation, condensation and temperature gradients on the stability of uniform and spreading surfactant-free thin liquid films on a heated or cooled substrates are studied by Burelbach *et al.* (1988), Joo *et al.* (1991), and López *et al.* (1996). From experimental viewpoint it is interesting to mention here the recent work of Sharma and Reiter (1996), where a direct comparison of theoretical predictions and experimental results on instabilities of various stages of dewetting of thin (< 60 nm) films on coated substrates are presented.

We consider the stability of horizontal two-layered liquid film which is evaporating in the presence of surfactant. The present study consists of three parts. In Part I (Danov *et al.*, 1997b), we used the lubrication approximation to derive the evolution equations for the thicknesses of the two liquid layers and to solve the surfactant diffusion problem. Linear analysis was performed in order to investigate the influence of the surfactant and the evaporation on the critical film thicknesses and the wavelength of the critical modes. In Part II (Danov *et al.*, 1997c) of this study, we applied the *linear stability analysis* to a typical system, consisting of water film, covered by light oil film. In particular, we choose water–hexane film attached to a solid (PVC) substrate. When only the water soluble surfactant is present in that system, it can adsorb at the water–hexane interface and it can decrease its tangential mobility. The upper hexane–vapour interface was not influenced by the surfactant. Numerical study of the linear stability of PVC/water/hexane film as been performed.

Here we perform *non-linear analysis* of the stability of an evaporating two-layered liquid film upon a heated solid substrate. Another typical system is considered: a heavy oil film, covered by a thin water layer. In particular, that is a tetrachlorethane–water film attached to plane PVC substrate. The surfactant is soluble in both liquid phases and can adsorb at both liquid–fluid interfaces. This study is organized as follows. In Section 2, the physical parameters of the system PVC/tetrachlorethane/water/vapour are discussed. Section 3 presents the equations of the non-linear initial value problem for one dimensional disturbances and the respective initial and boundary conditions. The numerical method for solving of the non-linear problem is described in Section 4. The numerical results and discussion are given in Section 5. Some details of the numerical scheme are described in the Appendix.

2. PHYSICAL PARAMETERS OF THE SYSTEM

There are numerous combinations between different types of liquid phases, surfactants and substrates. In order for our results to be physically realistic, we choose one typical configuration of the liquid phases: PVC/tetrachlorethane/water/vapor (P/T/W/V) and a typical set of parameters for low molecular surfactant.

In this case, the lower liquid phase is 1,1,2,2-tetrachlorethane (organic solvent of wide industrial use). It is heavier than water; it has a much higher boiling point (418 K) and is practically insoluble in water. The upper layer consists of water which is bounded above by its vapour. The surfactant (when present) is soluble in both liquid phases and can adsorb at both liquid interfaces (see Fig. 1). The values of the material parameters of the above system are listed in Table 1 for the saturation temperature of the water film (see Daubert and Danner, 1989).

If not mentioned specially, the temperature difference between the substrate surface, T_h, and the saturation temperature, T_s, is $\Delta T = 1°\mathrm{C}$. The value of the interfacial tension for tetrachlorethane–water interface is not available in the literature and we have estimated it by using the Antonov's rule (cf. Adamson, 1976). Thus, from the values of the surface tension $\sigma_{TV} = 2.62 \times 10^{-2}$ N/m for tetrachlorethane–vapour interface (Daubert and Danner 1989) and $\sigma_{WW} = 5.82 \times 10^{-2}$ N/m (for water–vapour interface) we obtain, $\sigma_1 = \sigma_{TW} \approx \sigma_{WW} - \sigma_{TV} = 3.20 \times 10^{-2}$ N/m. A similar estimate was also done for the interfacial tension temperature coefficient, $\mathrm{d}\sigma_1/\mathrm{d}T$, for tetrachlorethane–water interface.

To estimate the temperature coefficient of the water evaporation rate we use eq. (2) from Prosperetti and Plesset (1984),

$$J_T = \frac{\alpha \rho_v L}{T_s^{3/2}} \sqrt{\frac{M_W}{2\pi R_g}} \tag{1}$$

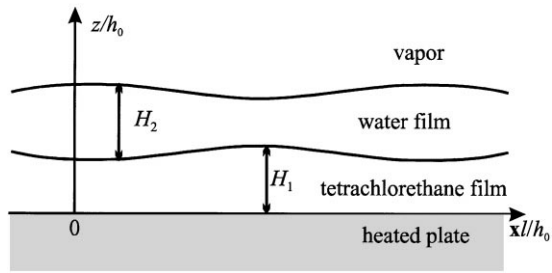

Fig. 1. Sketch of two-layered liquid film on a heated substrate.

Table 1. The physical parameters of 1,1,2,2-tetrachlorethane and water at the water saturation temperature, $T_S = 373\,\mathrm{K}$

Quantity	Tetrachlorethane (1)	Water (2)
Molecular weight, M (g/mol)	167.85	18.0
Liquid mass density, ρ (kg/m^3)	1468.0	973.5
Dynamic viscosity, η (Pa s)	6.41×10^{-4}	2.81×10^{-4}
Boiling temperature, T_S (K)	373.0	418.3
Thermal conductivity, λ (J/(ms K))	0.099	0.686
Latent heat of vaporization, L (J/kg)	—	2.27×10^6
Interfacial tension, σ (N/m)	3.20×10^{-2}	5.82×10^{-2}
Temperature coefficient of σ $(\partial\sigma/\partial T)$ (N/mK)	-7.5×10^{-5}	-1.94×10^{-4}

where the accommodation coefficient is taken to be unity, $\alpha \approx 1$. Thus, for the parameters $\rho_v = 0.585$ kg/m^3, $L = 2.27 \times 10^6$ J/kg, and $T_s = 373$ K, taken from Daubert and Danner (1989), we calculate $J_T = 3.414$ kg (s K m^2). The calculation of the Hamaker constants, appearing in the van der Waals dimensionless groups for this system, we perform as follows. We use the literature data of Izraelachvili (1992) for the Hamaker constants, $A_{PWP} = A_{PP} + A_{WW} - 2A_{PW} = 1.2 \times 10^{-20}$ J, $A_{WWW} = A_{WW} = 4.0 \times 10^{-20}$ J, $A_{PVP} = A_{PP} = 7.5 \times 10^{-20}$ J, and $A_{TVT} = A_{TT} = 5.5 \times 10^{-20}$ J (where W = water, P = PVC, and T = tetrachlorethane). Actually, the Hamaker constant A_{TT} is available only for CCl_4/vacuum/CCl_4 film, but we suppose that the van der Waals interaction for CCl_4 and for tetrachlorethane is similar. There is no data available in the literature for the Hamaker constants A_{TP} and A_{TW}. We used the approximate expressions (cf. Izraelachvili, 1992) $A_{PT} \approx \sqrt{A_{PP}A_{TT}} = 6.4 \times 10^{-20}$ J and $A_{TW} \approx \sqrt{A_{TT}A_{WW}} = 4.7 \times 10^{-20}$ J to estimate them. Finally, we obtain

$$A_1 = A_{PTW} = A_{PW} + A_{TT} - A_{TW} - A_{PT} - 3.8 \times 10^{-20}\,\mathrm{J} \tag{2}$$

$$A_2 = A_{TWV} = A_{WW} - A_{TW} = -0.7 \times 10^{-20}\,\mathrm{J} \tag{3}$$

$$A_i = A_{TW} - A_{PW} = 2.9 \times 10^{-20}\,\mathrm{J}. \tag{4}$$

Note that depending on the thickness of the two liquid layers, the respective van der Waals disjoining pressure can be either attractive or repulsive. For an illustration we have plotted in Figs. 2(a) and (b) the van der Waals disjoining pressure in the lower and the upper film

$$\Pi_1 = -\frac{A_1}{6\pi h_{\mathrm{low}}^3} - \frac{A_i}{6\pi(h_{\mathrm{low}} + h_0)^3},$$

$$\Pi_2 = -\frac{A_2}{6\pi h_0^3} - \frac{A_i}{6\pi(h_{\mathrm{low}} + h_0)^3} \tag{5}$$

(cf. Danov *et al.*, 1997b for details). Here with h_{low} and h_0 the thicknesses of the tetrachlorethane and the water film are denoted, respectively. The different curves correspond to a different thickness of the other liquid film. One sees that at small thicknesses the van der Waals disjoining pressure in the tetrachlorethane film is always repulsive, whilst in the water film it can be also attractive when the lower film is thinner than 10 nm. This means that the film rupture time will be influenced by the particular configuration of the two films in the final stage of the water film evaporation.

Typical parameters for different types of surfactants are available in Danov *et al.* (1997a). By default, we use the following values of the surfactant parameters, typical for low molecular surfactants (Table 2). Unless mentioned specially, the surfactant distribution coefficient is $m_{21} = 8$.

3. FORMULATION OF THE NON-LINEAR PROBLEM

3.1. *The governing equations*

We consider here only the case of one-dimensional perturbations of transitional symmetry. This assumption does not change the physics of the stability problem but the differential operators have their simplest form. Thus, the governing equations in dimensionless form, by Danov *et al.* (1997b), are simplified to read

3.1.1. *The compatibility equations for the films* 1 *and* 2

$$\frac{\partial H_1}{\partial \tau} = \frac{\partial}{\partial x}\left(H_1^3 \frac{\partial P_1}{\partial x}\right) - \frac{\partial}{\partial x}(H_1 U_1) \tag{6}$$

$$\frac{\partial H_2}{\partial \tau} = \frac{\partial}{\partial x}\left(H_2^3 \frac{\partial P_2}{\partial x}\right) - \frac{\partial}{\partial x}[H_2(U_1 + U_2)] - \frac{2\mathscr{K} + 1 + 2h_{12}\lambda_{212}}{2(\mathscr{K} + H_2 + H_1\lambda_{21})}. \tag{7}$$

Here τ and x are the dimensionless time and lateral coordinate, H_j and P_j $(j = 1, 2)$ are the dimensionless local thicknesses and pressures of the two layers, U_j are the respective interfacial velocities, $\mathscr{K}$ is the

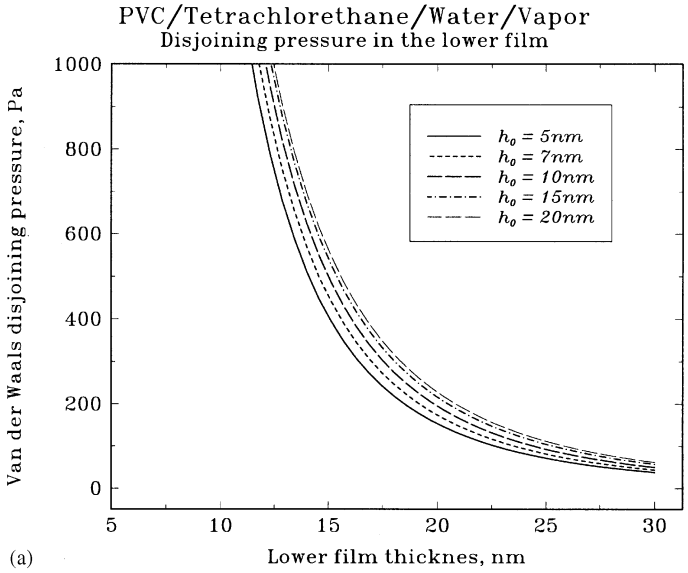

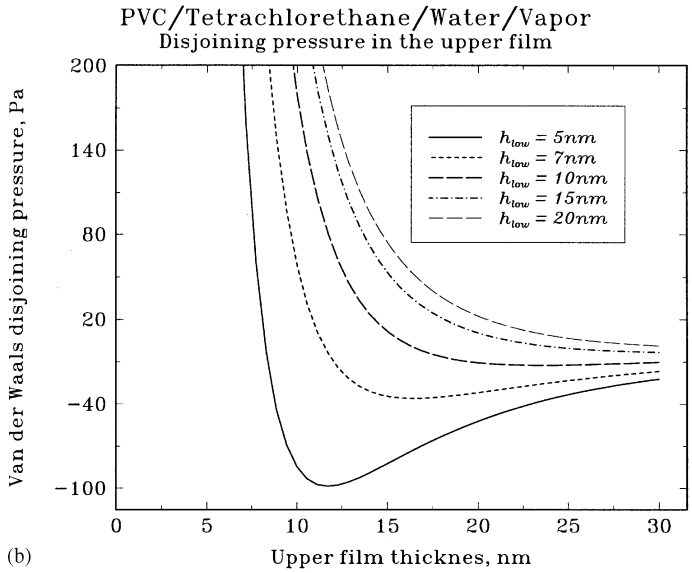

Fig. 2. Dependence of the dimensional van der Waals disjoining pressure on the film thickness: (a) for the tetrachlorethane film; the different curves correspond to different thickness, h_0, of the upper (water) film; (b) for the water film; the different curves correspond to different thickness, h_{low}, of the lower (tetrachlorethane) film.

degree of non-equilibrium number, and h_{12} and λ_{21} are the ratios of the initial thicknesses and the thermal conductivities of the two films.

3.1.2. *The total interfacial species transport equation*

$$\frac{\partial}{\partial\tau}[\Gamma_{12}G_1 + G_2 + \mathscr{Z}_2(H_2 + m_{21}H_1)C]$$
$$= \mathscr{B}\mathscr{Z}_2\frac{\partial}{\partial x}\left[(H_2 + m_{21}D_{12}H_1)\frac{\partial C}{\partial x}\right]$$
$$-\frac{\partial}{\partial x}\left[2\Gamma_{12}G_1U_1 + 2G_2U_2 - \mathscr{B}\left(\Gamma_{12}\mathscr{I}_1\frac{\partial G_1}{\partial x} + \mathscr{I}_2\frac{\partial G_2}{\partial x}\right)\right]$$
$$-\mathscr{Z}_2\frac{\partial}{\partial x}\left\{\left[H_2(U_1 + U_2) - H_2^3\frac{\partial P_2}{\partial x} + m_{21}\left(H_1U_1 - H_1^3\frac{\partial P_1}{\partial x}\right)\right]C\right\}. \quad (8)$$

The dimensionless numbers appearing here are: the ratios of the surfactant adsorptions at CMC, Γ_{12}, and the bulk diffusion coefficients, D_{12}, the surfactant capacity number, $\mathscr{Z}_2$, of the water film; the bulk diffusivity number, $\mathscr{B}$, and the surface diffusivity numbers, $\mathscr{Z}_j (j = 1, 2)$. In eq. (8), G_j and m_{21} are the

dimensionless adsorptions and the surfactant distribution coefficient, respectively (see Danov *et al.*, 1997b for more details).

3.1.3. *The normal stress balances at the film interfaces* 1 *and* 2

$$\eta_{12}P_1 = P_2 + \frac{\mathscr{W}_1}{6H_1^3} - \frac{\mathscr{W}_2}{6H_2^3} - \frac{\sigma_{12}}{4} \times\left[1 - \mathscr{S}_1\frac{\ln(1-\mathscr{G}_1G_1)}{\ln(1-\mathscr{G}_1)}\right]\frac{\partial^2 H_1}{\partial x^2} \tag{9}$$

$$P_2 = \frac{\mathscr{E}}{4}\frac{\mathscr{K}^2}{(\mathscr{K}+H_2+H_1\lambda_{21})^2} + \frac{\mathscr{W}_2}{6H_2^3} + \frac{\mathscr{W}_i}{6(H_1+H_2)^3} - \frac{1}{4}\left[1 - \mathscr{S}_2\frac{\ln(1-\mathscr{G}_2G_2)}{\ln(1-\mathscr{G}_2)}\right]\left(\frac{\partial^2 H_1}{\partial x^2} + \frac{\partial^2 H_2}{\partial x^2}\right). \tag{10}$$

Here η_{12} and σ_{12} denote the bulk viscosity ratio and the surface tension ratio; $\mathscr{W}_1$, $\mathscr{W}_2$, and $\mathscr{W}_i$ are the van der Waals numbers; $\mathscr{E}$ is the evaporation number and $\mathscr{S}_j$ and $\mathscr{G}_j$ ($j = 1, 2$) are dimensionless numbers characterizing the surfactant adsorption isotherm and surface equation of state.

3.1.4. *The tangential stress balance at the film interfaces* 1 *and* 2

$$\eta_{12}H_1\frac{\partial P_1}{\partial x} + \frac{\eta_{12}}{3H_1}U_1 + H_2\frac{\partial P_2}{\partial x} - \frac{1}{3H_2}(U_2 - U_1) = -\frac{2\mathscr{M}_1}{3}\frac{\partial}{\partial x}\left(\frac{\mathscr{K}+H_2}{\mathscr{K}+H_2+H_1\lambda_{21}}\right) - \frac{2\mathscr{A}_1}{3(1-\mathscr{G}_1G_1)}\frac{\partial G_1}{\partial x} + \frac{\mathscr{V}_1}{3}\frac{\partial}{\partial x}\left(G_1\frac{\partial U_1}{\partial x}\right) \tag{11}$$

$$H_2\frac{\partial P_2}{\partial x} + \frac{(U_2 - U_1)}{3H_2} = -\frac{2\mathscr{M}_2}{3}\frac{\partial}{\partial x}\left(\frac{\mathscr{K}}{\mathscr{K}+H_2+H_1\lambda_{21}}\right) - \frac{2\mathscr{A}_2}{3(1-\mathscr{G}_2G_2)}\frac{\partial G_2}{\partial x} + \frac{\mathscr{V}_2}{3}\frac{\partial}{\partial x}\left(G_2\frac{\partial U_2}{\partial x}\right) \tag{12}$$

$\mathscr{M}_j$ and $\mathscr{A}_j$ ($j = 1, 2$) are the thermal and the surfactant Marangoni numbers and $\mathscr{V}_j$ ($j = 1, 2$) are the surface viscosity numbers for the two liquid interfaces. All the notation and the dimensionless groups appearing in eqs (6)–(12) are described in detail by Danov *et al.* (1997b). The partial differential equations (6)–(8) together with the ordinary differential equations (9)–(12) and the respective adsorption isotherms [cf. eq. (49) and Danov *et al.* (1997b)] form an initial value problem which solution describes the evolution of the two-layer film on the heated substrate.

3.2. *Boundary conditions*

Two types of boundary conditions could be imposed depending on the particular physical configuration. Periodic boundary conditions can be used to study the behaviour of an infinite film corresponding to the more realistic case of a film which is much thinner than its lateral size. Besides, fixed boundary conditions can be used to investigate films of finite size as appear in experiment conditions (cf. De Wit *et al.*, 1994). In our numerical studies, we impose periodic boundary conditions for the film thicknesses H_1 and H_2, the pressures P_1 and P_2, the interfacial velocities U_1 and U_2, and the surfactant concentration C at the ends of the interval $x \in [0, 2\pi/k]$, with k being the respective wave number of the initial perturbation. In order to avoid confusion we emphasize that here and hereafter we use the term 'wave number' only for a brevity, to characterize the period of the initial disturbance of the film shape. Note that in the non-linear analyses the single initial mode degenerates in the process of the disturbance evolution.

3.3. *Initial conditions*

The initial conditions for the initial value problem we take from the linear stability analysis (cf. Danov *et al.*, 1997c)

$$H_j = H_{j,b}[1 + H_{j,f}\cos(kx)],$$

$$P_j = P_{j,b} + P_{j,f}\cos(kx), \quad U_j = U_{j,f}\sin(kx)$$

$$G_j = G_{j,b} + G_{j,f}\cos(kx), \quad C = C_b + C_f\cos(kx), \quad (j = 1, 2) \tag{13}$$

where the amplitudes of the initial perturbation are denoted by subscript f. Note that the perturbation amplitude $H_{2,f}$ of the evaporating surface is defined relative to the initial thickness of the upper layer, $H_{2,b} = 1$. The corresponding perturbation amplitude $H_{1,f}$ of the lower film thickness is defined relative to the constant h_{12}. The initial perturbations $H_{1,f}$ and $H_{2,f}$ can have both different and equal signs which corresponds to different coupling of the instability modes at the two interfaces. The case $H_{1,f}\,H_{2,f} < 0$ corresponds to the so-called squeezing mode perturbation, whilst $H_{1,f}\,H_{2,f} > 0$ gives the bending mode. In our calculations, we use initial perturbations in the symmetrical squeezing mode

$$H_{1,f} = -\frac{\varepsilon}{2}\frac{1}{h_{12}}, \qquad H_{2,f} = \varepsilon, \quad \varepsilon < 1 \tag{14}$$

and the complementary case of the anti-symmerical bending mode

$$H_{1,f} = \frac{\varepsilon}{h_{12}}, \quad H_{2,f} = 0, \quad \varepsilon < 1 \tag{15}$$

where the value of ε we fixed to 0.1 by default.

The squeezing mode is expected to be more effective in destabilising and rupture of the upper evaporating

film, but the bending mode disturbances can rupture the lower film. This is a novel element which is absent in the case of single film on a solid substrate (cf. Danov *et al.*, 1997a). The coupling of the modes at the different fluid interfaces can strongly influence the film stability.

In principle, the initial perturbation of the surfactant concentration, C_f, should be chosen independently from the initial perturbations of the film thickness. However, a general physical condition for the perturbation of the surfactant concentration is not available. Two limiting cases can be clearly distinguished:

(i) At slow or moderate evaporation, the surfactant diffusion to the film interfaces (and the respective adsorption) is so fast, that the initial disturbances of the film thicknesses can be considered as an evolution of the basic state. Then the concentration disturbance can be calculated from eqs (43) and (52) of Danov *et al.* (1997b) to be

$$C_f = -\frac{\mathscr{Z}_2(H_{2,f} + m_{21}h_{12}H_{1,f})C_b(0)}{\Gamma_{12}g_1 + g_2 + \mathscr{Z}_2(1 + m_{21}h_{12})} \quad (16)$$

where the quantities g_1, g_2, etc. are defined in Danov *et al.* (1997c).

(ii) The other limiting case is related to very fast perturbations of the film surfaces (e.g. for an intensive evaporation), when the initial perturbation of the surfactant concentration is negligible

$$C_f = 0. \quad (17)$$

In most cases (i) is realized, since the surfactant diffusion time is usually smaller than the evaporation time (the adsorption usually is a faster process than the surfactant diffusion). Only for high molecular surfactants and ultra-thin films, or very intensive evaporation the case (ii) seems to be more realistic.

Once the amplitudes of the film thickness and concentration perturbations are specified, we use the asymptotic of the linear analysis from Danov *et al.* (1997c) at zero time to calculate the inital perturbations for the pressure and the interfacial velocities.

3.4. *Critical parameters*

By definition, the time of the film rupture, τ_r, is reached when the local thickness of the one of the liquid layers becomes zero. Since the real time is scaled with the evaporation time of the upper layer, $\tau_r < 1$. However, in our case, the van der Waals disjoining pressure diverges when the film thickness approaches to zero. To avoid this mathematical complication and to prevent computational problems we introduce as a natural cut-off (for the film thickness) the size of the solvent molecule. For example, we consider that the water film has ruptured when its dimensional thickness becomes less than 2.5 Å, which is the diameter of the water molecule (cf. Adamson, 1976). We mention in advance that the introducing of such a cut-off does not change the rupture time in the framework of the numerical error.

The different modes correspond to different rupture times. The most unstable mode defines the critical time of film rupture, and the respective critical wave number,

$$\tau_{cr} = \min_k [\tau_r(k)]. \quad (18)$$

The corresponding basic state thickness of the upper layer 2 at the rupture time is defined as a critical thickness,

$$H_{cr} = H_{2,b}(\tau_{cr}). \quad (19)$$

The defining of critical thickness for the lower liquid film is not reasonable since its basic state thickness is not changing with time. Both τ_{cr} and H_{cr} are measure for the film stability for the given physical parameters.

4. THE NUMERICAL METHOD

The governing equations (6)–(8) are strongly non-linear partial differential equations (PDE). The explicit schemes like the two-step Lax–Wendroff scheme (cf. Fletcher, 1988), applied to that non-linear problem showed poor stability even for time step $\Delta\tau = 10^{-3}$. The reason was revealed from the results of the linear analysis (see Danov *et al.*, 1997c). Depending on the values of the two film thicknesses the PDE-system (or the corresponding system in the linear analysis) can become extremely stiff and then the explicit scheme of Lax–Wendroff does not work any more. We obtained much better results by using implicit Crank–Nicholson method (cf. Fletcher, 1988; Press *et al.*, 1992) in time with successive linearisation after the spatial discretization. Central differences in the spatial coordinates were used to obtain the discrete analogues of eqs (6)–(12) in conservative form. More details for the numerical scheme are presented in the Appendix.

For a given perturbation mode of wave number k, we subdivide the corresponding wavelength, $2\pi/k$ into $N = 50$ equal elements. As pointed out by Burelbach *et al.* (1988), the spatial-mesh effects are not important for $N > 20$ per wavelength when solving the compatibility equation for a single evaporating film. To maintain the stability we start with time step $\Delta\tau = 0.002$ and reduce it by a factor of 5 when the one of the film thickness becomes less than 20% of its initial value. We checked that the further decreasing of the initial time step practically does not change the result for the rupture time. Using the initial conditions, described in Section 3.3, we solve the initial value problem in time until one of the film ruptures. To find the critical thickness, we perform a minimisation of the rupture time with respect to the wave number.

5. NUMERICAL RESULTS AND DISCUSSION

Our aim here is to study the rupture mechanism of evaporating two-layered film and to estimate quantitatively how the presence of surfactant affects the film

critical parameters. When the liquid phases are surfactant-free, their interfaces can exhibit significant tangential mobility which influences the film rupture time and the critical wavelength of the perturbation. On the other hand, when surfactant is present at sufficiently high concentration, the interfacial elasticity and viscosity of the surfactant adsorption layers are usually high enough to suppress the tangential mobility of the liquid interfaces. We will consider the case of pure liquid phases, tangentially immobile film surfaces (a lot of surfactant), and the general case of intermediate surfactant concentration. Here and hereafter we use the physical parameters for PVC/tetrachlorethane/water/vapour film containing low molecular surfactant, as described in Section 2.

5.1. *Pure liquid phases and tangentially immobile interfaces*

Let us consider first the two limiting cases when the film is free from surfactant and the case of tangentially immobile surfaces (at high surfactant concentration). In both cases, the system of governing equations is simplified due to the discarding of the surfactant mass balance, eq. (8). When the film is free from surfactant

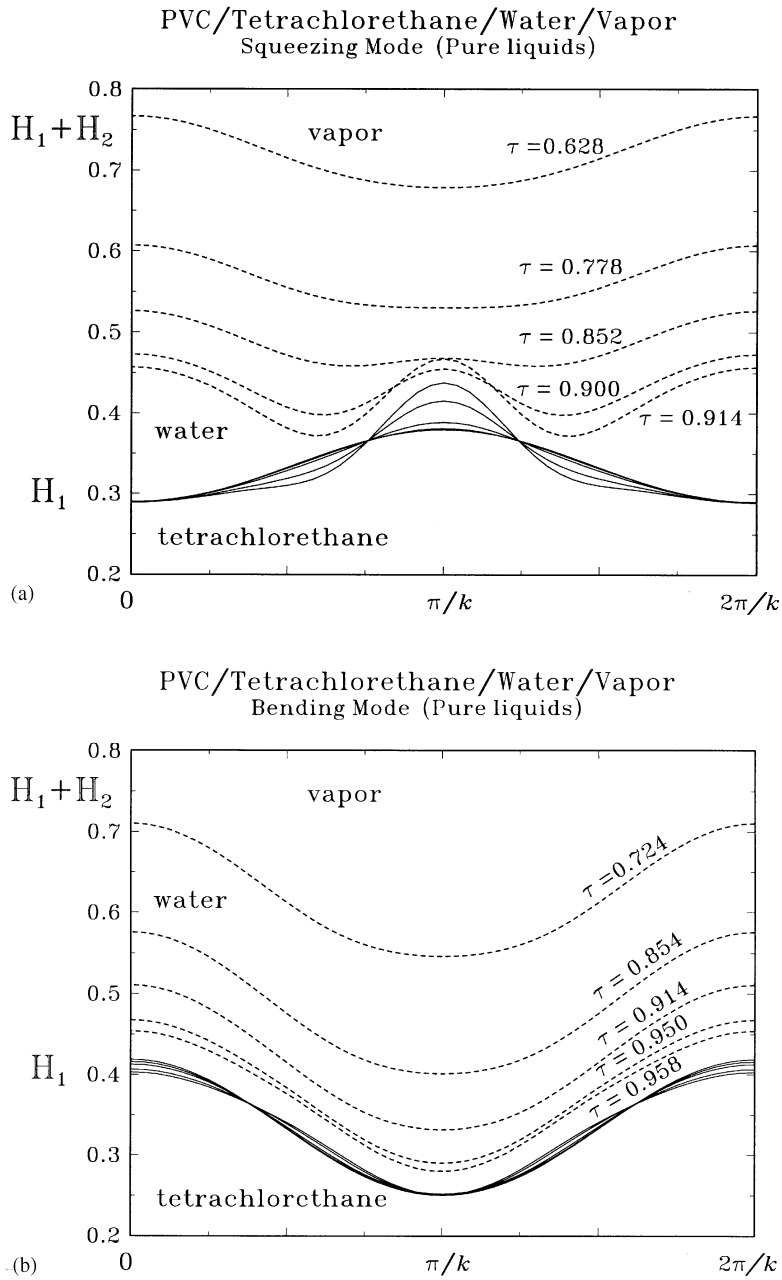

Fig. 3. Evolution of the interfaces of evaporating two-layered film: 'tetrachlorethane/water' on a PVC substrate: (a) squeezing mode with pure phases; (b) bending mode with pure phases; (c) squeezing mode with tangentially immobile interfaces; and (d) bending mode with tangentially immobile interfaces.

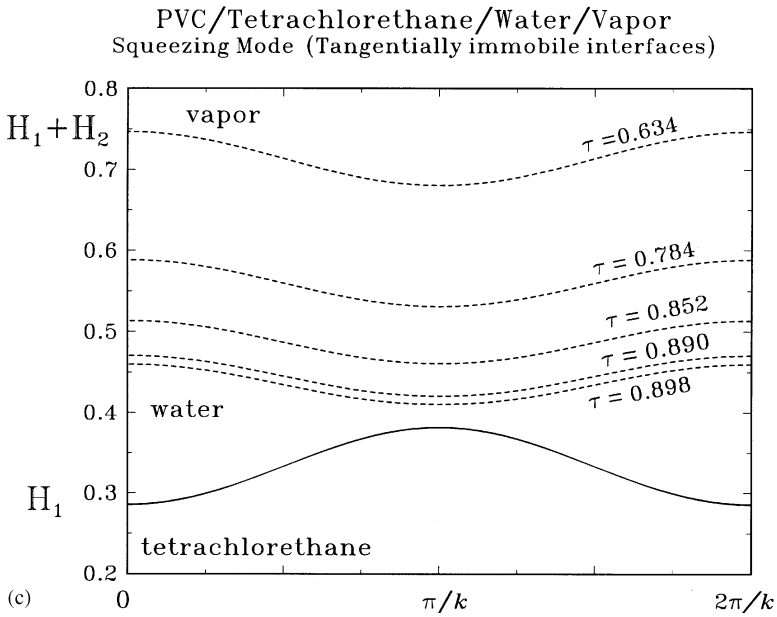

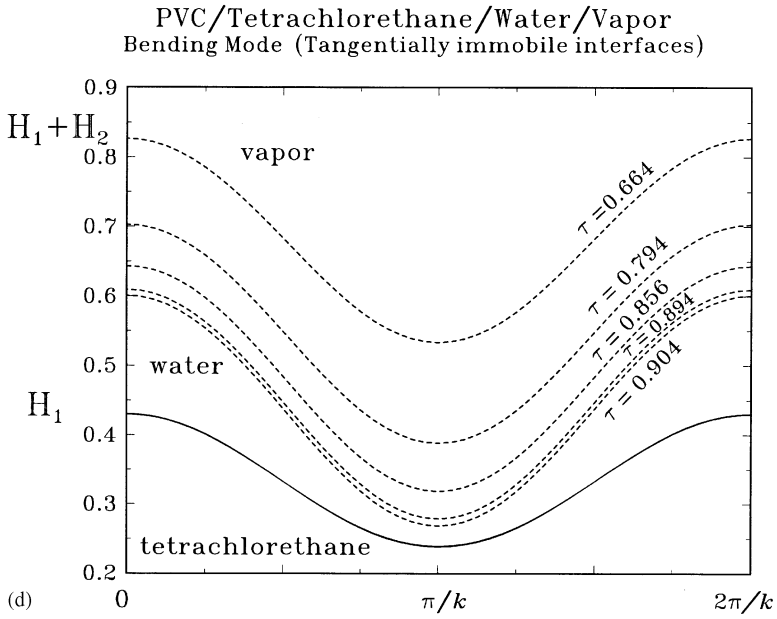

Fig. 3. (*Continued*).

all terms proportional to the surfactant adsorption (concentration) vanish. On the other hand, at high surfactant concentration both film surfaces (T/W and W/V) are saturated with surfactant, $G_1 = G_2 = 1$, and their interfacial velocities vanish, $U_1 = U_2 = 0$, due to the increased interfacial elasticity and viscosity of the adsorption layers. Hence the problem is additionally simplified due to elimination of the tangential stress balances, eqs (11) and (12).

We will illustrate first how the coupling of the perturbation modes at the two liquid interfaces, tetrachlorethane–water and water–vapour, influences the mechanism of the film rupture for the case of pure liquids. Figures 3(a) and (b) present a series of snapshots (taken at equal values of the minimal H_2) for the case of squeezing mode and bending mode, respectively (cf. Section 3.3). Here the initial thicknesses are: $h_0 = 15$ nm for the water film and $h_{low} = 5$ nm for the tetrachlorethane film. The temperature difference is $\Delta T = 0.1°C$. One sees that the water film in bending mode [Fig. 3(b)] is thinning slower than the same film in squeezing mode [Fig. 3(a)]. When the water film becomes thinner than 10 nm the squeezing mode degenerates into an asymmetric bending mode and causes additional perturbation of the tetrachlorethane film. The reason is that here the film interfaces are fully mobile and for these liquid phases (and the film thickness) the van der Waals disjoining pressure in the

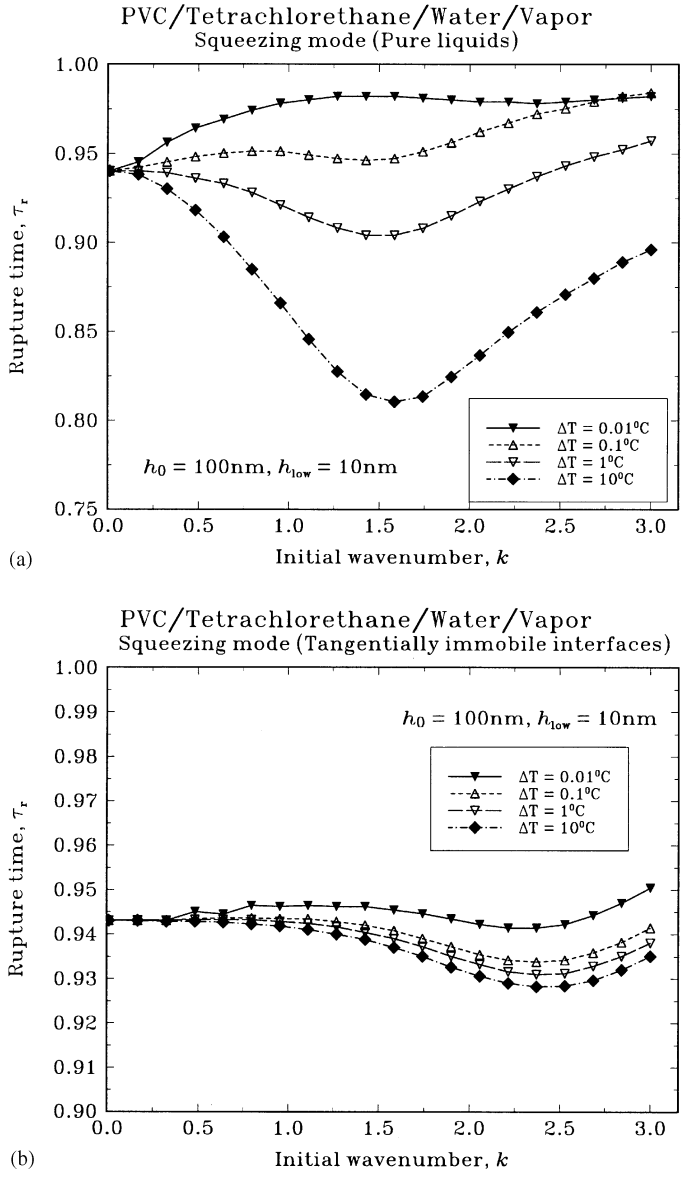

Fig. 4. Dependence of the rupture time on the initial wave number of the perturbation for evaporating two-layered film—tetrachlorethane–water on a PVC substrate: (a) for pure liquid phases; (b) for tangentially immobile interfaces. The initial film thicknesses are $h_0 = 100\,\text{nm}$ and $h_{\text{low}} = 10\,\text{nm}$. The different curves correspond to different temperature differeces, ΔT.

upper film is repulsive (cf. below with the case of tangentially immobile interfaces). However, we cannot conclude that the bending mode is always more stable than the squeezing one, since another our calculations [presented by Danov *et al.* (1997c) for water/hexane film] show that when the lower film is thin enough (about 5 nm) and upper film is thicker than 7 μm the bending mode perturbation upper film due to van der Waals instability. However, for the tetrachlorethane film the van der Waals pressure is repulsive [see Figs 2(a) and (b)] and such effect is not possible. We performed a similar comparison between the squeezing and bending initial mode for the case of tangentially immobile surfaces. The results are illustrated in Figs. 3(c) and (d), where the snapshots are taken for equal values of the minimal thickness, H_2. All other parameters are the same as in Figs 3(a) and (b). Again the water film in bending mode [Fig. 3(d)] is thinning slower than the same film in squeezing mode [Fig. 3(c)]. However, here the interfaces are both tangentially immobile and the squeezing mode does not degenerate into bending mode when the local thickness of the water film becomes small.

Figure 4(a) shows the dependence of the rupture time on the wave number of the initial perturbation for the case of pure liquids. Here we consider only film perturbations in squeezing mode and compare the

Table 2. Parameters for *low-molecular surfactant* in tetrachlorethane and water used in our calculations

Quantity	in tetrachlorethane or at T/W interface (1)	in water or at W/V interface (2)
$C_{k,\mathrm{CMC}}$ (mol/m^3)	8.0	1.0
$\Gamma_{k,\mathrm{CMC}}$ (mol/m^2)	2.0×10^{-6}	2.0×10^{-6}
η_k^S (Pa s m)	1.0×10^{-6}	1.0×10^{-6}
D_k (m^2/s)	1.3×10^{-10}	3.0×10^{-10}
B_k (m^2/s)	4.0×10^{-10}	4.0×10^{-10}
$\mathscr{G}_k$	0.95	0.95

relative film stability. The different curves correspond to different temperature differences ΔT. One sees that the critical wave number is very sensitive to the temperature difference. Since the liquids are pure, their interfacial tensions are high and for small temperature differences (e.g. $\Delta T = 0.01^\circ$C) only the waves of asymptotically small wave numbers ($k \to 0$) favour the film rupture. However, the situation is just the opposite in the case of intensive evporation, $\Delta T = 10^\circ$C, where the instabilities due to the solvent mass loss and the thermal Marangoni effect are dominating which increases the critical wave number and decreases the film rupture time.

The dependence of the critical rupture time on the initial thickness of the water film is presented in Fig. 5(a) for different values of ΔT. The thickness of the tetrachlorethane film is kept constant, $h_{\mathrm{low}} = 0.2\,\mu$m. The increasing of the rupture time with the increase of the water film thickness is explained by the increase of the thermal capacity of the water layer which suppresses the instability due to the evaporation mass loss. On the other hand, for the smaller thicknesses two factors increase the rupture time. These are the increased interfacial mobility of both the interfaces and the van der Waals disjoining pressure in the water film, which is repulsive in this case (for $h_{\mathrm{low}} = 0.2\,\mu$m).

Similarly as for pure liquid phases, we checked the dependence of the rupture time on the wave number of the initial perturbation for tangentially immobile surfaces. The results are presented in Fig. 4(b) where again the different curves correspond to different temperature differences, ΔT. Note that here the result is rather different from the case of pure phases [cf. Figs 4(a) and (b)]. Here the interfacial tensions are lower but the increased interfacial elasticity and interfacial viscosity due to the presence of surfactant suppress the short and moderate waves and make them not so effective in causing the film rupture. Thus, the rupture time is almost insensitive to the temperature difference, ΔT. This explains the result in Fig. 5(b), where the dimensionless critical thickness is plotted against the initial thickness of the water film for different values of ΔT. One sees that the curves practically coincide for all the film thicknesses between 10 and 1000 nm and the dimensionless critical thickness is not sensitive to ΔT when the film surfaces are tangentially immobile.

It is instructive to check how the thickness ratio, h_{12}, of the tetrachlorethane and the water film affects the film rupture time. This is illustrated in Figs 6(a) and 7(a) where the critical rupture time and the critical film thickness are plotted against the initial thickness of the water film for different values of h_{12}. One sees that the smaller the thickness of the tetrachlorethane film the larger the film rupture time. The reason is the increase of the thermal Marangoni number with the increase of the tetrachlorethane film thickness. Finally, the influence of the thickness ratio, h_{12}, on the rupture time and the critical thickness for the case of tangentially immobile interfaces is illustrated in Figs 6(b) and 7(b). One sees that the effect (and the explanation) is similar to the case of pure liquid phases.

5.2. *The effect of surfactant on the film stability*

In order to illustrate how the surfactant influences the stability of the evaporating tetrachlorethane–water film, we have plotted in Fig. 8(a) the rupture time as a function of the wave number. Here the initial film thicknesses are $h_0 = 100$ nm and $h_{\mathrm{low}} = 10$ nm, and the initial surfactant concentration is $C_0 = 5\times10^{-3}$. This figure shows that with an increase of the temperature difference, the critical wave number increases and for $\Delta T = 10^\circ$C the rupture time decreases with respect to the case of low ΔT. Even at such small concentration, the surfactant causes a slight solidification of the film interfaces thus suppressing the short waves. However for high-temperature differences the thermal Marangoni instability again contributes to the appearance of a minimum at finite wave numbers. Similar is the behaviour of the critical film thickness in the presence of surfactant. In order to emphasise the role of the surfactant and to facilitate the comparison between the three cases: pure phases; small and moderate surfactant concentrations; and tangentially immobile surfaces (a lot of surfactant), we have plotted in Fig. 8(b) the rupture time vs the wave number for $\Delta T = 10^\circ$C. Here the surfactant plays a stabilising role and increases the critical rupture time of the water film.

The influence of the surfactant concentration is studied in Figs 9(a) and (b), where the rupture time

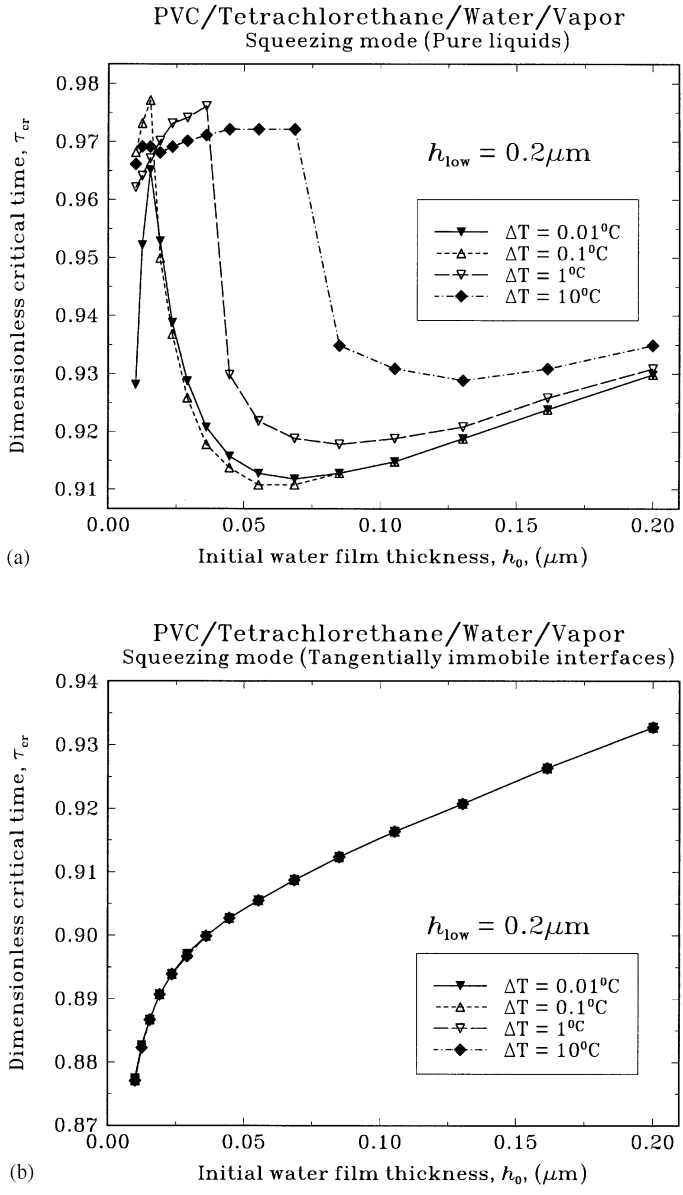

Fig. 5. Dependence of the dimensionless rupture time, τ_{cr}, on the initial thickness of the water layer, h_0, for evaporating two-layered film: tetrachlorethane–water upon a PVC substrate. The different curves correspond to different temperature differences, ΔT. The initial thickness of the tetrachlorethane film is $h_{low} = 0.2\,\mu$m. (a) for pure liquid phases; and (b) for tangentially immobile film interfaces.

and the critical film thickness are plotted as functions of the water layer thickness for different surfactant concentrations. Here the tetrachlorethane film thickness is $h_{low} = 0.1\,\mu$m. Note that the effect of surfactant is most pronounced for small ratios of the two film thicknesses, $h_{12} = h_{low}/h_0$. Then, increasing the surfactant concentration, the stability goes down because of the surface tension lowering [cf. Frumkin equations (17) from Danov *et al.* (1997b)]. It is seen that at these parameters there is an optimal thickness ratio (here $h_{12} \sim 0.2$–0.3), where the film is most stable. The position of the maximum of the critical rupture time vs h_0 depends on the surfactant concentration. We attribute it to a complex interplay between the Marangoni effect (which increases with the increase of h_0) and the surface viscosity effect (which decreases with the increase of h_0). We checked that when increasing the temperature difference this effect becomes less pronounced because then the thermocapillary effect is dominating.

Figures 10(a) and (b) present the effect of the surfactant solubility in the two liquid phases. Here the critical rupture time and the critical thickness are plotted against the surfactant distribution coefficient,

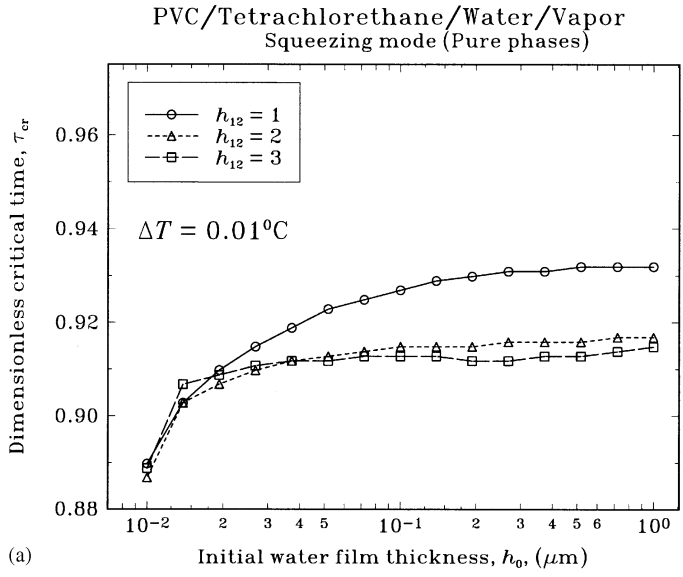

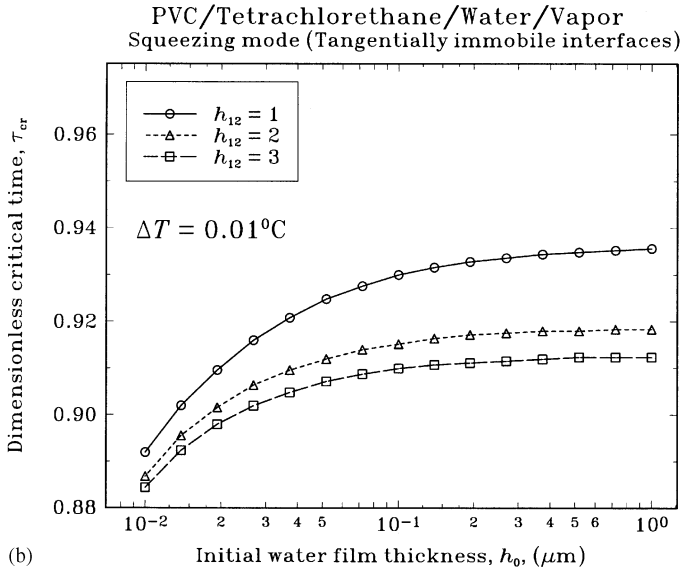

Fig. 6. Dependence of the dimensionless critical time, τ_{cr}, on the initial thickness of the water layer, h_0, for evaporating two-layered film: tetrachlorethane–water upon a PVC substrate. The different curves correspond to different values of the lower film thickness, h_{low} (or h_{12}). (a) Pure liquid phases; and (b) both film interfaces are tangentially immobile.

m_{21}. The different curves correspond to different temperature differences. Note that the critical rupture time exhibits a maximum as a function of m_{21}. The physical interpretation of this effect we propose is the following. The increase of the surfactant solubility in water (at fixed concentration, C_0) influences mainly the interfacial tension and the interfacial viscosity of T/W interface. By increasing the surfactant distribution coefficient the film stability goes up because of the increase of the interfacial viscosity effect and then goes down (for high m_{21}) due to the lowering of interfacial (T/W) tension. Thus, an optimal value of m_{21} exists where the growth rate of the instability due to the evaporation mass loss is minimal and the film stability is maximal. This explanation is in consonance with the fact that the position of the maximum depends strongly on the temperature difference (e.g. the intensity of the evaporation).

The results for the rupture times calculated from linear and non-linear stability analysis are compared in Figs 11(a)–(c) for the cases of pure liquids (a), tangentially immobile surfaces (b) and the case of intermediate surfactant concentrations (c). One sees that the differences are greatest for the case of pure liquid phases where at $\Delta T = 0.01°$C the linear analysis gives smaller rupture time than the non-linear

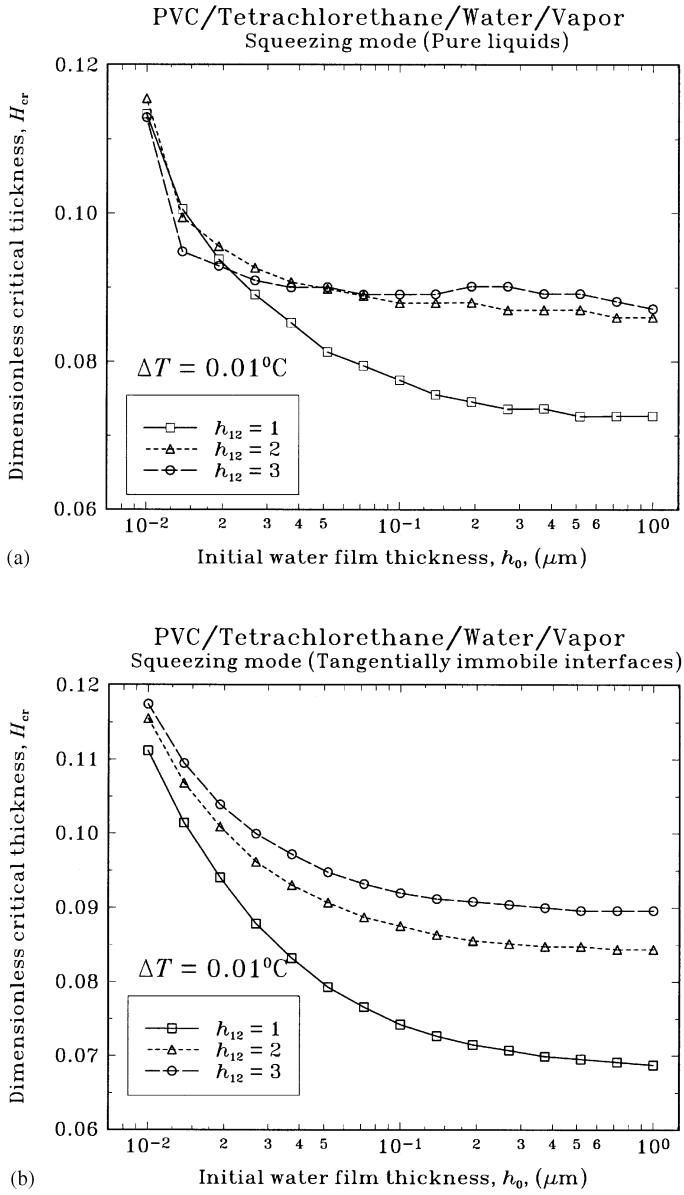

Fig. 7. Dependence of the dimensionless critical thickness, H_{cr}, on the initial thickness of the water layer, h_0, for evaporating two-layered film: tetrachlorethane–water upon a PVC substrate. The different curves correspond to different values of the lower film thickness, h_{low} (h_{12}). (a) Pure liquid phases, and (b) both film interfaces are tangentially immobile.

analysis. Usually, the non-linear analysis gives smaller rupture time than these from the linear analysis (see e.g. Williams and Davis, 1982; Burelbach *et al.*, 1988; De Wit *et al.*, 1994). However, in all these studies the van der Waals disjoining pressure is attractive (destabilizing factor) while in our case the van der Waals disjoining pressure is repulsive (stabilises the film). The latter, combined with the increased interfacial mobility (pure liquids) leads to longer rupture times at finite wave numbers. We can conclude that the non-linear analysis is more sensitive to the disjoining pressure effects than the linear analysis. Note that the addition of surfactant increases the film rupture time due to the solidification of the both liquid interfaces [cf. Figs 11(a)–(c)].

6. MAIN RESULTS AND CONCLUSIONS

Non-linear analysis is used to investigate the stability of evaporating two-layered liquid film upon a heated solid substrate in the presence of surfactant. The model accounts for the instabilities due to surface tension gradients created by disturbances in temperature and surfactant distribution, coupled by the solvent mass loss. Additionally, the role of the van der Waals surface force is also taken into

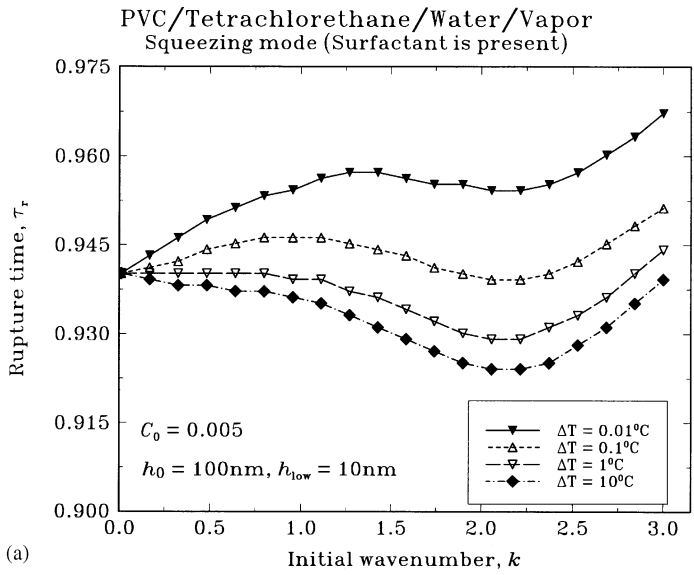

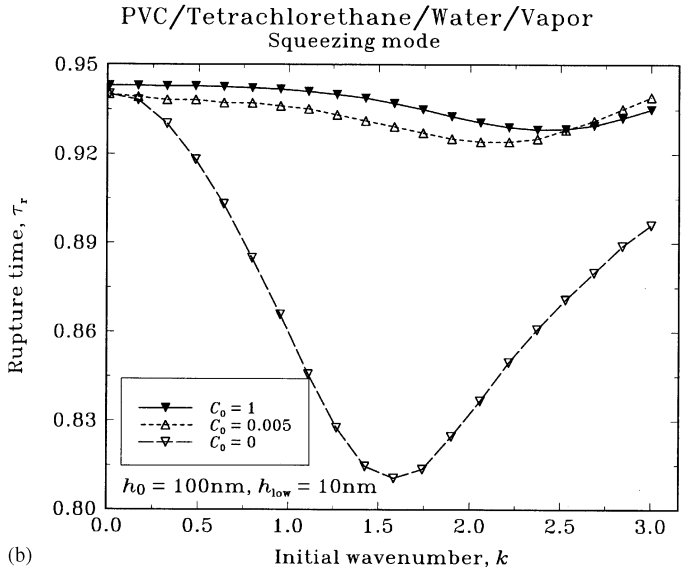

Fig. 8. Dependence of the rupture time on the initial wave number of the perturbation for evaporating two-layered film: tetrachlorethane–water on a PVC substrate. The initial film thicknesses are $h_0 = 100$ nm and $h_{low} = 10$ nm. (a) The different curves correspond to different temperature differences, ΔT. The initial surfactant concentration (dimensionless) is $C_0 = 5 \times 10^{-3}$. (b) The different curves correspond to different surfactant concentrations. The temperature difference is $\Delta T = 10°C$.

account. The main results of this study are the following:

• The stability of particular system (tetrachlorethane–water film upon a PVC substrate) against mechanical disturbances has been investigated. The role of different factors on the stability of two-layered film has been studied: the tangential mobility of the film surfaces; the intensity of the evaporation; the initial thicknesses of the two layers; the surfactant concentration; and the surfactant distribution coefficient. The coupling of the different modes at the two liquid surfaces is also examined.

• It is obtained that in most cases the film shape fluctuations in *squeezing mode* are more effective in the film rupture than these in *bending mode*.

• At high surfactant concentration, the rigidity of the interfacial adsorption layers suppress the short wave fluctuations. When the system is far from the saturation temperature, the instability due to the solvent mass loss and the thermal Marangoni instability are dominating the effect from the surfactant.

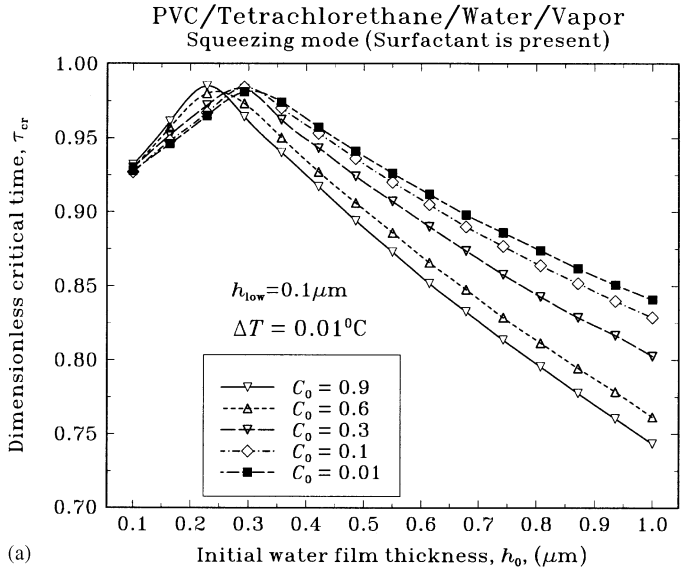

(a)

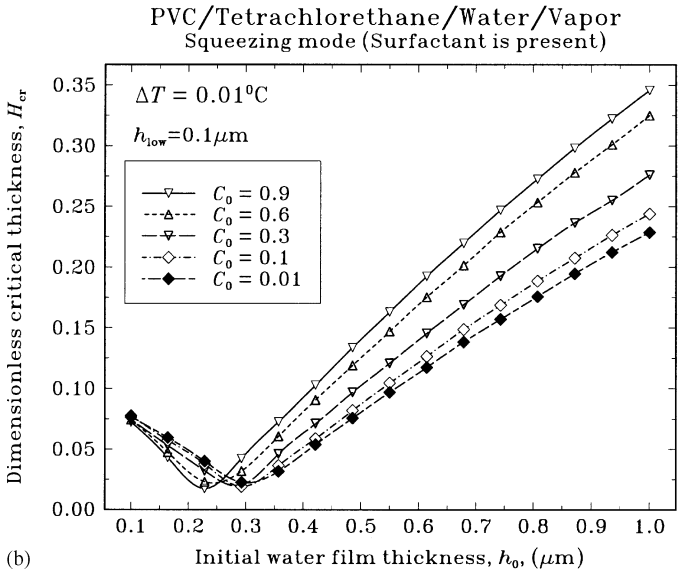

(b)

Fig. 9. Dependence of (a) the dimensionless critical time, τ_{cr}, and (b) the dimensionless critical thickness, H_{cr}, on the initial thickness of the water layer, h_0, for evaporating two-layered film: tetrachlorethane–water upon a PVC substrate in the presence of surfactant. The tetrachlorethane film thickness, h_{low} is fixed to 100 nm. The different curves correspond to different values of the surfactant concentration, C_0.

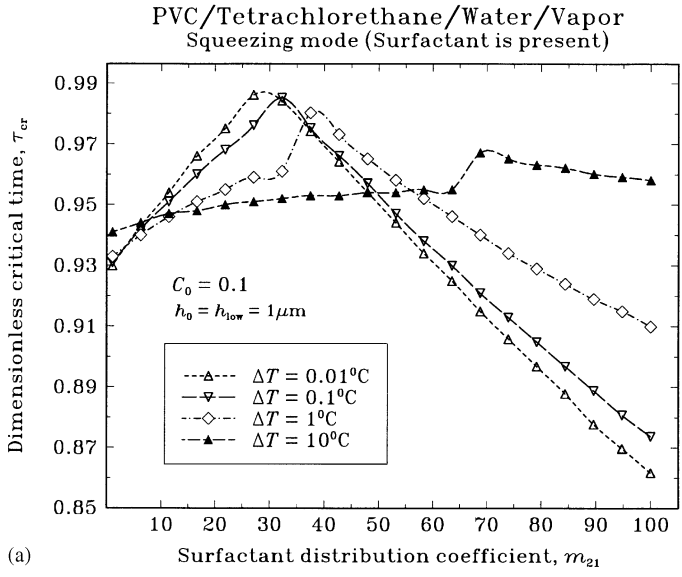

(a)

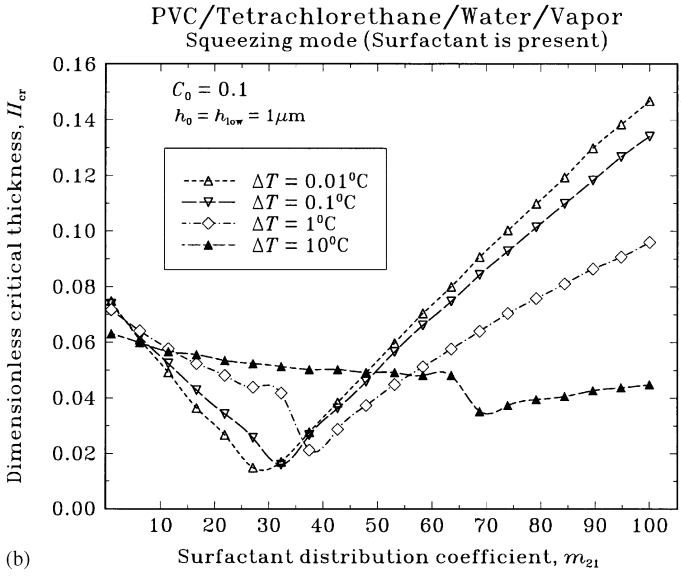

(b)

Fig. 10. Dependence of (a) the dimensionless critical time, τ_{cr}, and (b) the dimensionless critical thickness, H_{cr}, on the surfactant distribution coefficient, m_{21}, for evaporating two-layered film: tetrachlorethane–water on a PVC substrate in the presence of surfactant. The different curves correspond to different values of the temperature difference, ΔT. The initial film thickness are, $h_0 = h_{low} = 1\,\mu m$ and the surfactant concentration is $C_0 = 0.1$.

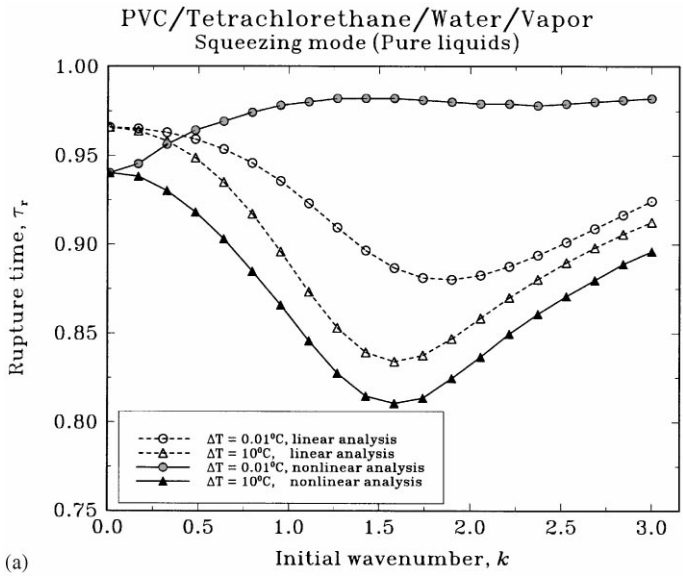

(a)

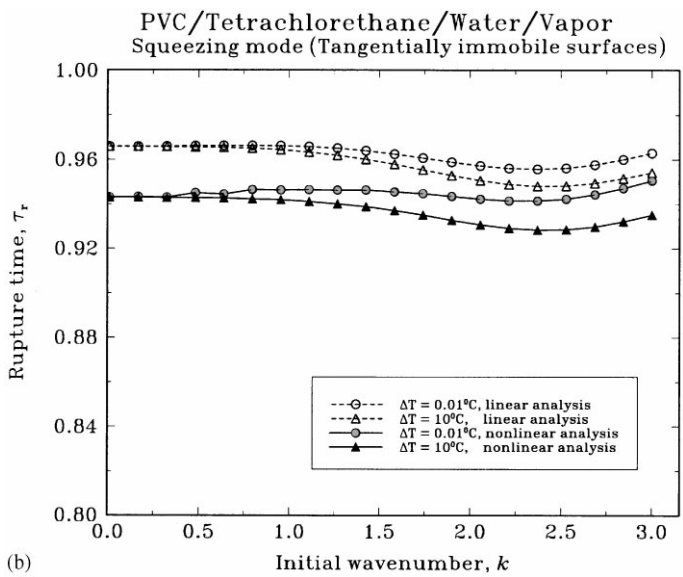

(b)

Fig. 11. Dependence of the rupture time on the initial wave number of the perturbation for evaporating two-layered film—tetrachlorethane–water on a PVC substrate: (a) for pure liquid phases; (b) for tangentially immobile interfaces; (c) in the presence of surfactant, $C_0 = 0.005$. The initial film thicknesses are $h_0 = 100$ nm and $h_{low} = 10$ nm. The different curves correspond to two different temperature differences, ΔT, calculated by non-linear analysis (the solid curves) and by linear analysis (the dashed curves).

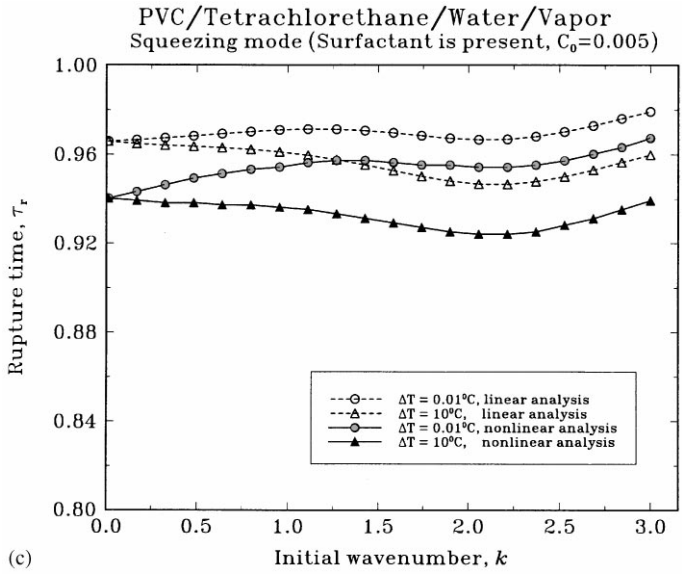

(c)

Fig. 11. (*Continued*).

• The surfactant distribution coefficient is an important factor, which influences the film stability in a complex manner. The film stability exhibits a maximum as a function of the surfactant solubility in the water phase which is due to the interplay between the increasing of the interfacial viscosity and the lowering of the interfacial tension for T/W interface.

• The non-linear effects in the instability growth are most essential for the case of pure phases where the mobility of the liquid interfaces is highest. The increasing of the surfactant concentration decreases the difference between the results from the linear and non-linear stability analysis.

Acknowledgments

This work is financially supported by the Volkswagen-Stiftung. The authors gratefully acknowledge the support of their collaborative research.

REFERENCES

Adamson, A. W. (1976) *Physical Chemistry of Surfaces*. Wiley, New York, U.S.A.

Burlbach, J. P., Bankoff, S. G. and Davis, S. H. (1988) Nonlinear stability of evaporating/condensing liquid films. *J. Fluid Mech.* **195**, 463–494.

Chang, H.-C. (1987) Evolution of nonlinear waves on vertically falling films—a normal form analysis. *Chem. Engng Sci.* **42**, 515–533.

Danov, K. D., Alleborn, N., Raszillier, H. and Durst, F. (1998a) The stability of evaporating thin liquid films in the presence of surfactant: I. Lubrication approximation and linear analysis. *Phys. Fluids* **10**(1), 131–143.

Danov, K. D., Paunov, V. N., Alleborn, N., Raszillier, H. and Durst, F. (1998b) Stability of the evaporating two-layered liquid film in the presence of surfactant: I. The equations of lubrication approximation. *Chem. Engng Sci.* **53**, 2809–2822.

Danov, K. D., Paunov, V. N., Stoyanov, S. D., Alleborn, N., Raszillier, H. and Durst, F. (1998c) Stability of the evaporating two-layered liquid film in the presence of surfactant: II. Linear analysis. *Chem. Engng Sci.* **53**, 2823–2837.

Daubert, T. E. and Danner, R. P. (1989) *Physical and thermodynamical properties of pure chemicals*. Data Compilation, Hemisphere, New York, U.S.A.

De Wit, A., Gallez, D. and Christov, C. I. (1994) Nonlinear evolution equations for thin liquid films with insoluble surfactants. *Phys. Fluids* **6**, 3256–3266.

Fletcher, C. A. J. (1988) *Computational Techniques for Fluid Dynamics*, Vol. 1. Springer, Berlin.

Gallez, D. (1994) Non-linear stability analysis for animal cell adhesion to solid support. *Colloids Surfaces* **2**, 273–280.

Hatziavramidis, D. (1992) Stability of thin evaporating/condensing films in the presence of surfactant. *Int. J. Multiphase Flow* **18**, 517–530.

Izraelachvili, J. N. (1992) *Intermolecular and Surface Forces*, 2nd Ed. Academic Press, London.

Joo, S. W., Davis, S. H. and Bankoff, S. G. (1991) Long-wave instabilities of heated falling films: two-dimensional theory of uniform layers. *J. Fluid Mech.* **230**, 117–146.

Lee, J.-J. and Mei, C. C. (1996) Stationary waves on an inclined sheet of viscous fluid at high Reynolds and moderate Weber numbers. *J. Fluid Mech.* **307**, 191–229.

López, G., Bankoff, S. G. and Miksis, M. J. (1996) Non-isothermal spreading of a thin liquid film on an inclined plane. *J. Fluid Mech.* **324**, 261–286.

Paulsen, F. G., Pan, R., Bousfield, D. W. and Thompson, E. V. (1996) The dynamics of bubble/particle attachment and the application of two disjoining film rupture models to flotation. *J. Colloid. Interface Sci.* **178**, 400–410.

Press, W. H., Teukolsky, S A., Vetterling, W. T. and Flannery, B. P. (1992) *Numerical Recipes in Fortran. The Art of Scientific Computing*, 2nd Ed. Cambridge University Press, Cambridge.

Prosperetti, A. and Plesset, M. S. (1984) The stability of an evaporating liquid surface. *Phys. Fluids* **27**, 1590–1602.

Ramaswamy, B., Chippada, S. and Joo, S. W. (1996) A full-scale numerical study of interfacial instabilities in thin-film flows. *J. Fluid Mech.* **325**, 163–194.

Sharma, A. and Reiter, G. (1996) Instability of thin polymer films on coated substrates: rupture, dewetting, and drop formation. *J. Colloid. Interface Sci.* **178**, 383–399.

Williams, M. B. and Davis, S. H. (1982) Nonlinear theory of film rupture. *J. Colloid. Interface Sci.* **90**, 220–228.

Yiantsios, S. G. and Higgins, B. G. (1991) Rupture of thin films: nonlinear stability analysis. *J. Colloid. Interface Sci.* **147**, 341–350.

APPENDIX: APPLICATION OF CRANK-NICHOLSON METHOD TO THE NON-LINEAR STABILITY PROBLEM

Following Press *et al.* (1992) we represent eqs (1)–(3) in the form

$$\frac{H_{1,j}^{n+1} - H_{1,i}^{n}}{\Delta\tau} = \frac{1}{2}[\mathbf{L}_1^{(n)} + \mathbf{L}_1^{(n+1)}] \tag{A1}$$

$$\frac{H_{2,i}^{n+1} - H_{2,i}^{n}}{\Delta\tau} = \frac{1}{2}[\mathbf{L}_2^{(n)} + \mathbf{L}_2^{(n+1)}] \tag{A2}$$

$$Z_{1,i}^{n}\frac{H_{1,i}^{n+1} - H_{1,i}^{n}}{\Delta\tau} + Z_{2,i}^{n}\frac{H_{2,i}^{n+1} - H_{2,i}^{n}}{\Delta\tau} + Z_{3,i}^{n}\frac{C_i^{n+1} - C_i^{n}}{\Delta\tau} = \frac{1}{2}[\mathbf{L}_3^{(n)} + \mathbf{L}_3^{(n+1)}] \tag{A3}$$

where

$$Z_{1,i}^{n} = \mathscr{Z}_2 m_{21} C_i^{n}, \quad Z_{2,i}^{n} = \mathscr{Z}_2 C_i^{n},$$

$$Z_{3,i}^{n} = \mathscr{Z}_2(H_{2,i}^{n} + m_{21}H_{1,i}^{n}) + \Gamma_{12} g_{1,i}^{n} + g_{2,i}^{n} \tag{A4}$$

$$g_{1,i}^{n} = \frac{C_{12}m_{21}(1-\mathscr{G}_1)}{[(1-\mathscr{G}_1)C_{12}m_{21} + \mathscr{G}_1 C_i^{n}]^2},$$

$$g_{2,i}^{n} = \frac{1-\mathscr{G}_2}{(1-\mathscr{G}_2 + \mathscr{G}_2 C_i^{n})^2}. \tag{A5}$$

Here the indices, i and n denote space and time coordinate, respectively; $\mathbf{L}_k$, $k = 1, 2, 3$, represent the right-hand side of eqs (6)–(8), discretised in space. Equations (A1)–(A3) are coupled with the discrete form of eqs (9)–(12). To obtain finally a system of linear algebraic equations, only the quantities coming from the discretisation of the spatial derivatives are kept in the next time step, $(n + 1)$. The other (non-linear) terms are marked as coefficient functions and are estimated from the previous time step, n. A similar numerical scheme has been successfully used for solving of the compatibility equation for the evolution of diffusion dimples. For small enough time step, $\Delta\tau$, that scheme is satisfactory stable for such class of non-linear initial value problems.

Thus, for each spatial point, i, we obtain 7 algebraic equations for the quantities:

$$\begin{aligned}
&a_{j,1}H_{1,j-1}^{n+1} + a_{j,2}H_{1,i}^{n+1} + a_{j,3}H_{1,i+1}^{n+1} \\
&\quad + a_{j,4}H_{2,i-1}^{n+1} + a_{j,5}H_{2,i}^{n+1} + a_{j,6}H_{2,i+1}^{n+1} \\
&\quad + a_{j,7}P_{1,i-1}^{n+1} + a_{j,8}P_{1,i}^{n+1} + a_{j,9}P_{1,i+1}^{n+1} \\
&\quad + a_{j,10}P_{2,i-1}^{n+1} + a_{j,11}P_{2,i}^{n+1} + a_{j,12}P_{2,i+1}^{n+1} \\
&\quad + a_{j,13}U_{1,i-1}^{n+1} + a_{j,14}U_{1,i}^{n+1} + a_{j,15}U_{1,i+1}^{n+1} \\
&\quad + a_{j,16}U_{2,i-1}^{n+1} + a_{j,17}U_{2,i}^{n+1} + a_{j,18}U_{2,i+1}^{n+1} \\
&\quad + a_{j,19}C_{1,i-1}^{n+1} + a_{j,20}C_{1,i}^{n+1} + a_{j,21}C_{1,i+1}^{n+1} = b_j, \\
&\quad (j = 1, \ldots, 7).
\end{aligned} \tag{A6}$$

All the coefficients a_{ij} and b_j are estimated using the information from the previous time step n or from the initial conditions $n = 1$. Equations (A6) form a band diagonal linear system which is solved very efficiently with the subroutines BANDEC and BANBKS from Numerical Receips (cf. Press *et al.*, 1992) to get the solution for the next time step.